

Prediction of Infarct Growth Based on Apparent Diffusion Coefficients: Penumbra Assessment without Intravenous Contrast Material¹

Charlotte Rosso, MD
Nidiyare Hevia-Montiel, PhD
Sandrine Deltour, MD
Eric Bardin, PhD
Didier Dormont, MD, PhD
Sophie Crozier, MD
Sylvain Baillet, PhD
Yves Samson, MD

Purpose:

To compare predicted and final infarct lesion volumes determined by processing apparent diffusion coefficient (ADC) maps derived at admission diffusion-weighted (DW) magnetic resonance (MR) imaging in patients with acute stroke and to verify that predicted areas of infarct growth reflect at-risk penumbral regions based on recanalization status.

Materials and Methods:

The French legislation waived the requirement for informed patient consent for the described research, which was based on patient medical files. However, patients and/or their relatives were informed that they could decline to participate in the research. Authors tested a semi-automated proprietary image analysis procedure in 98 patients with middle cerebral artery (MCA) stroke by modeling infarct growth on DW imaging-derived ADC maps. Predicted infarct growth (PIG) areas and predicted infarct volumes were correlated with final observed data. In addition, the effect of MCA recanalization on the correlation between predicted and observed infarct growth volumes was qualitatively assessed.

Results:

Predicted and final infarct volumes ($\rho = 0.828$; 95% confidence interval [CI]: 0.753, 0.882; $P < .0001$) and infarct growth volumes ($\rho = 0.506$; 95% CI: 0.342, 0.640; $P < .0001$) were significantly correlated. Visual comparative examination revealed satisfactory qualitative consistency between predicted and follow-up lesion masks. In patients without MCA recanalization, PIG did not differ significantly from final observed infarct growth (median PIG obtained with 0.93 ADC ratio cutoff [PIG_{ratio}] of 27.1 cm³ vs median infarct growth of 19.8 cm³, $P = .17$). MCA recanalization revealed an overestimation of PIG (median PIG_{ratio} of 24.8 cm³ vs median infarct growth of 12 cm³, $P = .005$), suggesting that the PIG area was part of ischemic penumbra.

Conclusion:

Data show the feasibility of identifying at-risk ischemic tissue in patients with acute MCA stroke by using semiautomated analysis of ADC maps derived at DW imaging, without intravenous contrast material-enhanced perfusion-weighted imaging.

© RSNA, 2008

Supplemental material: <http://radiology.rsna.org/cgi/content/full/2493080107/DC1>

¹ From AP-HP-Urgences Cérébro-Vasculaires (C.R., S.D., S.C., Y.S.), Laboratoire de Neurosciences Cognitives et Imagerie Cérébrale (C.R., N.H., E.B., D.D., S.B.), and AP-HP-Service de Neuroradiologie (D.D.), Université Pierre et Marie Curie; and Centre de Neuroimagerie de Recherche (E.B.), Hôpital Pitié-Salpêtrière, 47-83 Bd de l'Hôpital, 75013 Paris, France. Received January 16, 2008; revision requested March 18; revision received April 9; accepted July 2; final version accepted July 11. Supported in part by the "Programme Hospitalier de Recherche Clinique EVAL-USINV" (No. AOM 03 008). C.R. supported in part by the JNLF (Journées de Neurologie de Langue Française) Association. N.H. supported by the CONACYT/SFERE training programs from the Mexican and French Ministries of Foreign Affairs. Address correspondence to C.R. (e-mail: charlotte.rosso@gmail.com).

Although predicting the risk of further infarct growth (IG) is critical to therapeutic decision making, it remains a challenging task in patients who have had an acute stroke (1). Thus, a fast, standardized, and accurate tool dedicated to image analysis could prove useful and eventually might contribute to the redefining of essential therapeutic windows (2) or the designing of proof-of-concept therapeutic trials (3–5). The mismatch of perfusion imaging and diffusion imaging findings has been considered an imaging surrogate for ischemic penumbra and has been proposed as an indicator of the area of IG (6,7). Hence, investigators in a recent multicenter study (2,8) found that perfusion imaging–diffusion imaging mismatch predicts favorable responses to thrombolysis when early reperfusion occurs, although the theoretic and practical values of this mismatch have been challenged in several studies (9–13) and more recently by the negative outcomes of the Desmoteplase in Acute Ischemic Stroke Trial (14) and the limited conclusions drawn from the Echoplanar Imaging Thrombolytic Evaluation Trial (15).

These considerations led us to investigate whether the risk of IG could be predicted from diffusion-weighted (DW) magnetic resonance (MR) imaging data only. The concept is based on the mild decrease in the apparent diffusion coefficient (ADC), which has been demonstrated in the ischemic penumbra and in tissues at risk of infarction in

experimental (16,17) and human (9,18,19) studies. It was shown, however, that local voxel-based ADCs overlap in penumbral and normal tissues (18,19). To overcome this, we developed an image-processing model that mimics the process of IG with use of ADC data. This technique works by means of the integration of voxels around the ischemic core according to local and regional ADC measures and additional shape regularity constraints. A brief technical description of this technique is described in Appendix E1 (<http://radiology.rsnajnl.org/cgi/content/full/2493080107/DC1>).

Preliminary results (20) have demonstrated the feasibility of the voxel integration method. In the present study, we validated the technique in 98 patients with acute middle cerebral artery (MCA) stroke by using DW images acquired within 6 hours after stroke onset. Therefore, the purpose of our study was to compare the predicted and final infarct lesion volumes determined by processing ADC maps derived at admission DW MR imaging and to verify that predicted areas of IG reflect at-risk penumbral regions based on recanalization status.

Materials and Methods

Patients

A patent (No. PCT/FR2007/001111) is pending for the image analysis procedure described herein. All authors except one (S.C.) are equally represented

in this patent, which is chaired by Centre National de la Recherche Scientifique as the academic institution. All imaging and clinical data were generated during routine clinical work-up of the patients in the Salpêtrière Cerebrovascular Emergency Department and were retrospectively extracted for the purposes of this study. Therefore, and according to French legislation, the requirement for explicit informed patient consent was waived. However, the regulation concerning electronic filing was respected, and both the patients and their relatives were informed that the patient's data might be used in retrospective clinical research studies. None of them declined such use of the data.

The data of consecutive patients with acute nonlacunar MCA stroke were selected by three authors (C.R., S.D., S.C., 4–15 years experience in cerebrovascular medicine). Patient data were included on the basis of the following criteria: The patient had undergone admission MR imaging within the first 6 hours after stroke onset and follow-up MR imaging within at least the first following week without symptomatic hemorrhagic transformation. According to

Advances in Knowledge

- Apparent diffusion coefficient (ADC)-based prediction of infarct growth (IG) with use of a semiautomated and standardizable method is feasible and does not require intravenous contrast material administration.
- Predicted final infarct size and IG correlate with observed infarct size at follow-up.
- ADC-defined tissue at risk for infarct may represent ischemic penumbra, as it is partially spared with complete arterial recanalization.

Implications for Patient Care

- ADC-based prediction of IG has the potential to enable the identification of at-risk tissue regions without intravenous contrast material administration.
- The described IG prediction technique might be of future value when penumbral assessment is required but there are contraindications to contrast-enhanced perfusion imaging—for example, in clinical trials designed to extend the time window for intravenous thrombolytic therapy.

Published online before print
10.1148/radiol.2493080107

Radiology 2009; 250:184–192

Abbreviations:

ADC = apparent diffusion coefficient
DW = diffusion weighted
IG = infarct growth
IQR = interquartile range
MCA = middle cerebral artery
PIG = predicted IG
PIG_{ADC} = PIG determined by using $740 \times 10^{-6} \text{ mm}^2/\text{sec}$ absolute ADC cutoff
PIG_{ratio} = PIG determined by using 0.93 ADC ratio cutoff
V1 = infarct volume at admission
V2 = final infarct volume

Author contributions:

Guarantor of integrity of entire study, Y.S.; study concepts/study design or data acquisition or data analysis/interpretation, all authors; manuscript drafting or manuscript revision for important intellectual content, all authors; manuscript final version approval, all authors; literature research, C.R., N.H., Y.S.; clinical studies, C.R., S.D., S.C., Y.S.; statistical analysis, C.R., Y.S.; and manuscript editing, C.R., S.B., Y.S.

See Materials and Methods for pertinent disclosures.

the routine clinical protocol at our institution, the patients may have received tissue plasminogen activator intravenously within an expanded 5-hour time window. Expanding the time window for intravenous lytic agent administration is a common practice at many centers where MR imaging is a first-line imaging procedure; however, the prediction technique introduced herein was not considered in the clinical decision of whether to perform thrombolysis.

Three authors (S.D., S.C., 8 and 15 years experience in cerebrovascular medicine, respectively; D.D., neuroradiologist with 25 years experience) in consensus classified the intracranial artery occlusions into four categories on the basis of the admission MR angiography data: (a) internal carotid artery terminus occlusions, (b) simultaneous intracavernous carotid artery and MCA trunk occlusions, (c) MCA trunk occlusions, and (d) MCA trifurcation branch occlusions. The MCA recanalization status was assessed independently on the follow-up MR angiograms by at least two observers (S.D. and D.D. for all patients, S.C. when needed to reach a consensus in cases of disagreement).

MR Imaging Methods

MR imaging was performed by using a 1.5-T whole-body MR unit (Signa Horizon EchoSpeed; GE Healthcare, Buc, France) with enhanced gradient hardware for echo-planar imaging. DW, fluid-attenuated inversion-recovery, and intracranial time-of-flight MR angiography examinations were performed. Axial fast fluid-attenuated inversion-recovery imaging was performed with 8800/140/2200 (repetition time msec/echo time msec/inversion time msec), 5-mm-thick sections with a 1.5-mm intersection gap, a 256×256 matrix, and a 240×240 -mm field of view. Axial isotropic spin-echo echo-planar DW imaging entailed the acquisition of 24 5-mm-thick sections with an intersection gap of 0.5 mm, 2825/98.9 (repetition time msec/echo time msec), a 280×210 -mm field of view, and a 96×64 matrix. Baseline T2-weighted and DW MR images were acquired in 40 seconds by using a diffusion gradient

of 1000 sec/mm^2 . Time-of-flight MR angiography was performed by using a vascular time-of-flight by spoiled gradient-recalled acquisition, 2825/92.6 (repetition time msec/effective echo time msec), an axial section thickness of 1.4 mm, a 256×192 matrix, a 240×180 -mm field of view, a 20° flip angle, 36 locations per slab, and an acquisition time of 2 minutes 39 seconds.

Quantitative ADC maps were generated by using dedicated commercially available software (Funtool 2; GE Healthcare). ADC map thresholds of $(150 \text{ to } 1200) \times 10^{-6} \text{ mm}^2/\text{sec}$ were set to remove voxels contaminated by partial volume effects from cerebrospinal fluid (8).

Region Volumes Defined by Using MR Imaging

The infarct volume at admission (V1) was defined as the abnormal hyperintense area seen on the initially obtained DW images ($b = 1000 \text{ sec/mm}^2$) and was measured by means of interactive manual outlining at an Advantage Windows workstation (GE Healthcare). The final infarct volume (V2), the abnormal hyperintense area seen on the follow-up DW images, was also measured. IG was defined as the difference between V2 and V1. These operations were performed by one author (C.R.), who was blinded to the clinical data.

Prediction of IG

General principles.—The image-processing algorithm was developed by three authors (N.H., E.B., S.B., 4–10 years experience in image-processing techniques); a technical description of this algorithm is detailed in Appendix E1 (<http://radiology.rsna.org/cgi/content/full/2493080107/DC1>) (20). Briefly, the prediction of IG (Fig 1) based on the admission ADC map is ruled by an image model that mimics the natural history of IG by iteratively accumulating voxels around the admission core of the infarct. The growth model is controlled by the minimization of a global energy index, which is predominantly based on the evaluation of regional ADCs complemented by local ADC indexes and controls the regularity of the surface envelope of the lesion to

avoid erratic growth patterns. The average ADC of the growing infarct model tends to increase as the volume increases radially away from the core of the ischemic focus toward more peripheral regions. The growth process is automatically terminated when the global energy of the lesion model is minimized, and this occurs essentially when the regional ADC within the final infarct model reaches a prespecified cutoff value.

To determine the optimal ADC cutoff values, a preliminary study was performed by one author (C.R.) (21) by screening a series of ADCs close to $748 \times 10^{-6} \text{ mm}^2/\text{sec}$ and ADC ratios close to 0.91, which were reported in the retrospective study of Oppenheim et al (9) as the best thresholds for predicting tissue viability in the setting of hyperacute MCA stroke. The best performances in predicting tissue viability were rendered with an ADC of $740 \times 10^{-6} \text{ mm}^2/\text{sec}$ and an ADC ratio of 0.93. The normalized ADC cutoff value was defined as 0.93 times the average contralateral normal ADC determined in a spherical volume of interest of 0.73 cm^3 placed manually in the deep white matter of the noninfarcted hemisphere. In this study, both the optimal absolute ADC cutoff value and the normalized ADC cutoff value were similar to those reported by Oppenheim et al (9).

Practical implementation.—One author (C.R.) processed and analyzed the admission DW images and ADC maps by using dedicated in-house software at a Linux workstation (Dell Precision 670; Dell France, Montpellier, France). In each patient, the growth model was initialized by using an estimation of the infarct core, depicted as the abnormal bright area on the admission DW images, which was segmented by using an interactive thresholding approach. These seed volumes and V1 were found to be highly correlated ($r = 0.987$, $P < .0001$), indicating the reproducibility of admission lesion measurements obtained by using two software solutions and distinct image-processing environments. The DW imaging infarct core was automatically transferred onto the ADC map, and the growth model was run automatically to yield a predicted infarct volume. Two predicted

infarct volumes were determined: one by using the 740×10^{-6} mm²/sec ADC cutoff and one by using the 0.93 ADC ratio cutoff. Similarly, two volumes of predicted IG (PIG)—defined as the difference between the predicted infarct volume and V1—were derived: the PIG determined by using the 740×10^{-6} mm²/sec ADC cutoff (PIG_{ADC}) and the PIG determined by using the 0.93 ADC ratio cutoff (PIG_{ratio}). Image analysis took approximately 10 minutes per case at a standard personal computer workstation, and the only operator-dependent step was the segmentation of the infarct core volume on the admission DW image.

Data and Statistical Analyses

The descriptive statistics used were means \pm standard deviations, or medians and interquartile ranges (IQRs). Group comparisons were performed by using Mann-Whitney *U* nonparametric tests because the empirical probability distributions of the measures were not normal. The predicted and observed infarct sizes and growth volumes in the entire group of patients were compared by using Spearman nonparametric correlation rank tests (MedCalc for Windows, version 9.3.2.0; MedCalc Software, Mariakerke, Belgium). Regression lines were com-

puted. PIG volumes were compared with observed IG volumes by using the Bonferroni multiple-comparison test.

Qualitative indications of the spatial correspondence between the predicted and final infarct regions were assessed by visually comparing the predicted infarct masks estimated from the admission and follow-up DW images. The follow-up DW images were screened for supplementary lesions in and outside the involved MCA territory distant from the predicted infarct lesion.

Patients were subsequently assigned to one of two groups: patients with complete or partial MCA recanalization ($n = 70$) and patients without MCA recanalization ($n = 27$), as identified at follow-up MR angiography. For one patient, follow-up MR angiography data were not interpretable because of poor quality. Group comparisons were performed by using Mann-Whitney *U* nonparametric tests because the empirical probability distributions of the measures were not normal. Regression lines of IG versus PIG were computed, and the slopes and intercepts of these lines were compared between the recanalization and no recanalization patient groups. IG versus PIG measures were also compared within the recanalization and no recanalization groups, with

distinctions between complete recanalization ($n = 50$) and partial recanalization ($n = 20$) subgroups made by using Wilcoxon signed rank tests.

Finally, we studied the effect of the timing of the admission and follow-up MR examinations on the accuracy of the predictions. First, V1 and V2 were correlated with the timing of the admission and follow-up MR examinations, respectively, by using Spearman nonparametric correlation rank tests. The patients were additionally separated into two groups according to the median time of their admission MR examination: early or late—that is, before or after the median time of admission. The Spearman rank coefficients for correlations between PIG and observed IG were compared between the “early” and “late” groups. The same analysis was applied for follow-up MR imaging, with the early group imaged before the sample median delay after stroke onset and the late group imaged afterward.

Results

Descriptive Analysis

Ninety-eight consecutive patients (median age, 60 years; age range, 26–84

Figure 1

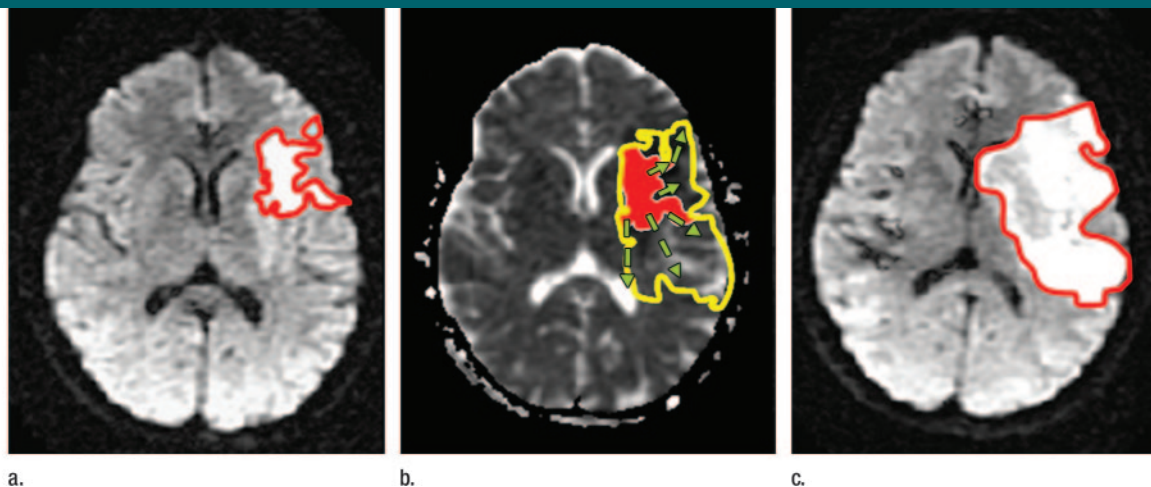


Figure 1: Prediction of MCA IG in 49-year-old man who had MCA infarct with MCA trunk occlusion, without recanalization, at admission MR imaging performed 104 minutes after stroke onset. **(a)** On DW image obtained at admission, the initial infarct lesion is outlined in red. **(b)** On ADC map obtained at admission, the lesion is shaded red. The region-growing model progressively expands (arrows) this region until the predicted volume (outlined in yellow) is reached. **(c)** On follow-up DW image, the final measured infarct volume, outlined in red, is visible as a hyperintense region. In this patient, the admission infarct volume was small (16.3 cm³) and the predicted volume (84.1 cm³) was an underestimation of the final infarct size (126.9 cm³). At follow-up MR imaging, the MCA is not recanalized.

years) were selected for the study. The median baseline National Institutes of Health Stroke Scale (NIHSS) score was 15 (IQR, 10–19) at admission and 10 (IQR, 5–17) 24 hours later. Sixty-four (65%) patients received tissue plasminogen activator intravenously.

Admission MR imaging was performed a median of 2.3 hours (IQR, 1.8–3.0 hours) after stroke onset. Fifty-nine (60%) of the 98 lesions were lateralized to the left, and 39 (40%) were lateralized to the right; these data were consistent with the statistics in the clinical database of patients who underwent thrombolysis in our department. Intracranial artery occlusion was detected at admission MR angiography in 86 (88%) patients. Sixteen (19%) occlusions were classified as internal carotid artery terminus occlusions; 11 (13%), as simultaneous intracavernous carotid artery and MCA trunk occlusions; 35 (41%), as MCA trunk occlusions; and 21 (24%), as MCA trifurcation branch occlusions. For three patients, the type of intracranial artery occlusion could not be assessed because of movement artifacts.

Follow-up MR imaging was performed a median of 1.2 days (IQR, 1.0–1.8 days) after the admission examination. Follow-up MR imaging revealed complete MCA recanalization in 50 (51%) of the 98 patients and partial recanalization in 20 (20%). Time of admission MR imaging (median, 2.3 vs 2.2 hours; $P = .35$), baseline NIHSS score (median, 15 vs 16; $P = .56$), and baseline serum glucose level (median, 6.2 vs 6.8 mmol/L; $P = .18$) were similar between the recanalization and no recanalization patient groups, respectively; however, these groups were significantly different in age (median age, 58.5 vs 61.0 years; $P = .04$). Nineteen (70%) of 27 patients in the no recanalization group and 45 (64%) of 70 patients in the recanalization group were treated with tissue plasminogen activator. Descriptive volume parameter measurements are detailed in Table 1.

Correlation Analysis

V2 correlated highly with both volume predicted with the 0.93 ADC ratio cutoff ($\rho = 0.828$ [95% confidence interval:

0.753, 0.882]; $P < .0001$) and volume predicted with the 740×10^{-6} mm²/sec absolute ADC cutoff ($\rho = 0.777$ [95% confidence interval: 0.684, 0.845]; $P < .0001$). IG correlated with both PIG_{ratio} ($\rho = 0.506$ [95% confidence interval: 0.342, 0.640]; $P < .0001$) and PIG_{ADC} ($\rho = 0.479$ [95% confidence interval: 0.310, 0.640]; $P < .0001$). These results are illustrated in Figure 2.

IG volumes (mean \pm standard deviation, 32.6 cm³ \pm 47.1) were similar to PIG_{ratio} values (33.8 cm³ \pm 38.6, $P > .05$) and smaller than PIG_{ADC} values (61.7 cm³ \pm 72.3, $P < .0001$) (repeated-measures analysis of variance and Bonferroni multiple-comparison test), indicating that use of the infarct model parametrized with the absolute ADC cutoff led to strong overestimations of the observed IG. Figure 2 also illustrates these results with comparisons of the slopes between the regression lines (mean slope, 0.80 \pm 0.09 for PIG_{ratio} vs 0.41 \pm 0.05 for PIG_{ADC} ; $P = .0002$).

Visual comparative examination revealed satisfactory qualitative consistency between the predicted and follow-up lesion masks. The predicted and final observed infarct regions were overlapping in the entire patient sample ($n = 98$). At follow-up MR imaging, new supplementary lesions distant from the predicted regions were detected in the MCA territory in nine (9%) cases and outside the involved MCA territory in six (6%) cases (three each in posterior and anterior cerebral artery territories).

Effects of Recanalization

Consistent with the hypothesis that arterial recanalization contributes to sparing of ADC-defined at-risk tissue, the mean slope of the regression lines for PIG_{ratio} in Figure 3 was larger in the no recanalization patient group ($n = 27$) (1.25 \pm 0.23) than in the complete or partial recanalization group ($n = 70$) (0.59 \pm 0.07, $P = .0004$). Similar results were obtained for PIG_{ADC} (mean slope, 0.55 \pm 0.10 for no recanalization group vs 0.28 \pm 0.04 for complete or partial recanalization group; $P < .0001$).

Furthermore, in the patients with complete or partial recanalization, the observed IG was smaller than the PIG

Table 1

Descriptive Volume Parameter Measurements

Parameter (cm ³)*	Mean [†]	Median [‡]
V1	34.2 \pm 34.6	20.5 (9.1–55.8)
V2	66.8 \pm 69.7	48.6 (17.5–98.0)
PV_{ratio}	65.0 \pm 64.8	42.8 (15.9–99.4)
PV_{ADC}	92.9 \pm 99.6	57.5 (28.1–118.5)
IG	32.6 \pm 47.1	13.5 (4.5–44.1)
PIG_{ratio}	33.8 \pm 38.6	24.3 (4.9–43.9)
PIG_{ADC}	61.7 \pm 72.3	39.0 (19.8–67.8)

* PV_{ADC} = volume predicted by using the 740×10^{-6} mm²/sec absolute ADC cutoff, PV_{ratio} = volume predicted by using the 0.93 ADC ratio cutoff.

[†] Mean values \pm standard deviations.

[‡] Numbers in parentheses are IQRs.

(median IG of 12 cm³ vs median PIG_{ratio} of 24.8 cm³, $P = .005$). Conversely, the difference was not significant in the patients with no recanalization (median IG of 19.8 cm³ vs median PIG_{ratio} of 27.1 cm³, $P = .17$). More detailed stratification (Fig 4) revealed that the difference was even larger when the analysis was restricted to patients with complete recanalization ($n = 50$) (median IG of 6.9 cm³ vs median PIG_{ratio} of 22.6 cm³, $P = .005$). The difference was not significant in the patients with partial recanalization ($n = 20$) (median IG of 29.3 cm³ vs median PIG_{ratio} of 26.8 cm³, $P = .33$).

Effect of Imaging Time

V1 did not correlate with time of admission MR imaging ($\rho = 0.03$, $P = .71$), and V2 did not correlate with time of follow-up MR imaging ($\rho = 0.05$, $P = .74$). In addition, the predictive value of the method was similar between the patients with early and those with late admission MR imaging times, with similar Spearman rank correlation coefficients ($\rho = 0.455$ for early group vs $\rho = 0.573$ for late group, $P = .44$). Similar results were obtained when the patients were grouped according to the median delay to follow-up MR imaging ($\rho = 0.458$ for early group vs $\rho = 0.475$ for late group, $P = .92$).

Discussion

The reported study results demonstrate the feasibility of DW imaging–

based prediction of IG in patients with acute (<6 hours) MCA stroke with use of proprietary ADC map analysis that does not require intravenous contrast agent administration. We found the predicted and observed IG volumes to be significantly correlated in a large series of patients with a wide range of infarct and IG volumes. Furthermore, we found that ADC-predicted areas of IG were likely to represent penumbral regions because they were largely spared in the setting of arterial recanalization (11). The described image analysis technique is based on an algorithm in which the IG is simulated and that relies on the mild ADC decrease that occurs in the ischemic penumbra,

as established in animal (16,17) and retrospective human (9,18,19) studies. The modeled IG proceeds from the core of the ischemic focus toward more peripheral areas and is guided by using local and regional indexes. This may explain why the method works despite the overlap between penumbral and normal ADCs at the voxel level (18,19). Interestingly, the best predictions were made by using ADC cutoff values that are similar to those reported in human retrospective studies (9,18). Also in accordance with these studies, the growth model parametrized by using a normalized ADC cutoff value performed slightly better than did the model parame-

trized by using an absolute ADC threshold.

The described IG prediction method has several advantages: First, it requires the use of only DW imaging, the key MR examination for evaluating acute stroke. The method requires neither the use of perfusion-weighted imaging, which is not always feasible during emergency screening of thrombolysis candidates, nor the intravenous administration of contrast agents, which might be contraindicated, especially in cases of severe renal insufficiency. Second, this IG prediction technique is semiautomatic: Operator intervention is restricted to the interactive drawing of the infarct seen at admission. Finally,

Figure 2

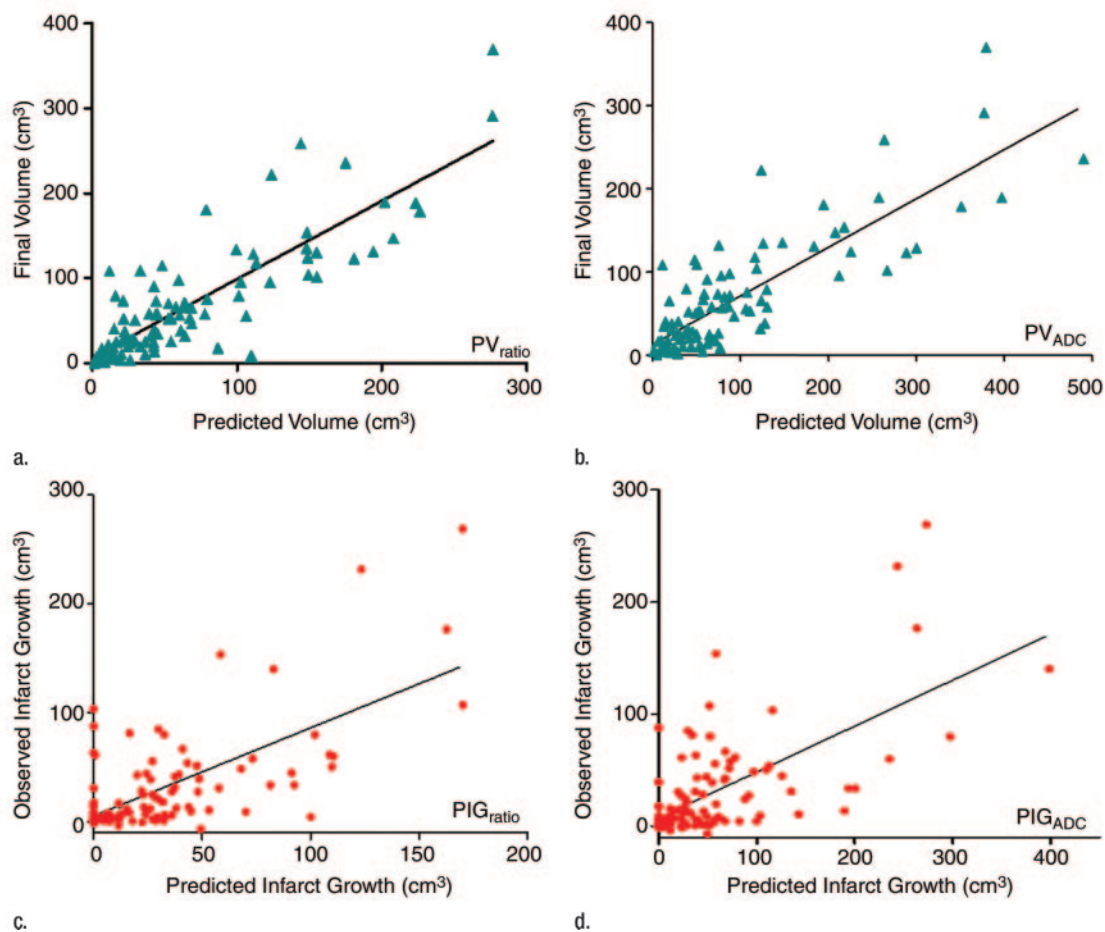


Figure 2: Correlation coefficients for absolute and normalized ADC cutoff values. Scatterplots of (a) V2 versus infarct volume predicted with 0.93 ADC ratio cutoff ($\rho = 0.828, P < .0001, y = 7 + 0.92x$), (b) IG versus PIG_{ratio} ($\rho = 0.506, P < .0001, y = 5.2 + 0.80x$), (c) V2 versus infarct volume predicted with 740×10^{-6} mm^2/sec absolute ADC cutoff ($\rho = 0.777, P < .0001, y = 12.5 + 0.58x$), and (d) IG versus PIG_{ADC} ($\rho = 0.479, P < .0001, y = 7.3 + 0.41x$) are shown.

Figure 3

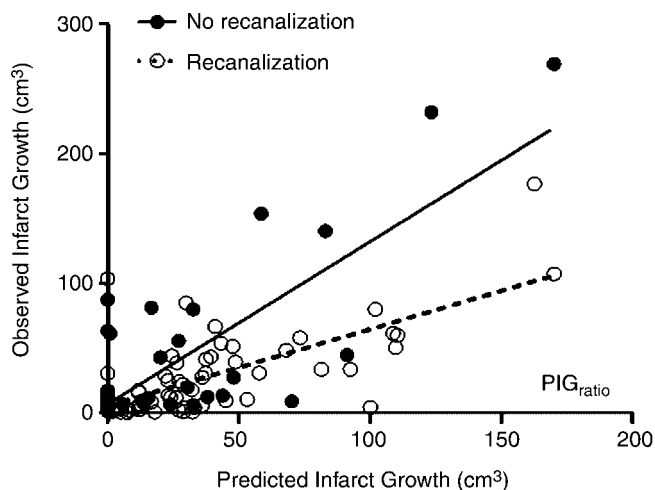


Figure 3: Effects of recanalization, as illustrated on scatterplot of IG versus PIG_{ratio} for recanalization (○) versus no recanalization (●) patient groups. The slope of the regression line for patients without recanalization is significantly higher than that for patients with recanalization (mean slope, 1.25 ± 0.23 vs 0.59 ± 0.07 ; $P < .0001$).

Figure 4

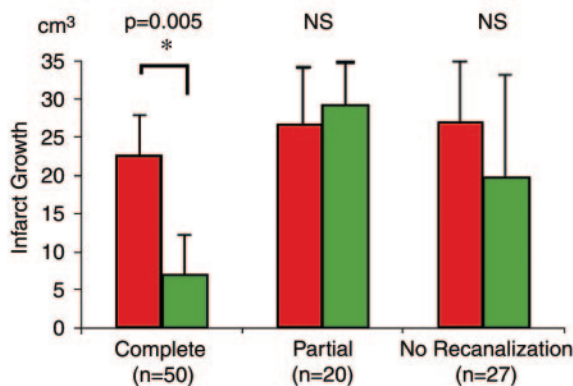


Figure 4: Effects of recanalization, as illustrated on bar graph of IG and PIG_{ratio} in patients with complete, partial, and no recanalization. Predicted (red) and observed (green) IG values are illustrated. IG is significantly different (*) from PIG_{ratio} in the complete recanalization group but not in the partial recanalization ($P = .33$) and no recanalization ($P = .17$) groups. *NS* = nonsignificant difference.

Table 2

Correlations between Final Infarct Volume and Acute Perfusion Abnormalities 12 Hours after Stroke Onset in Previous Studies

Study*	Hemodynamic Parameter	Correlation Coefficient
Parsons et al (22)	rCBF	0.91
Schellinger et al (23)	MTT	...
Barber et al (24)	rMTT	0.83
Beaulieu et al (25)	TTP	0.86
Rordorf et al (26)	rCBV	0.84
Parsons et al (27)	MTT	0.51
Shih et al (28)	T_{max}	0.78
	T_{max}	0.49
Thijs et al (29)	MTT	0.92
Rose et al (30)	MTT	0.84
	CBF	0.87
Derex et al (31)	TTP	0.35
Schellinger et al (32)	TTP	0.64
Röther et al (33)	TTP	0.76

Note.—The hemodynamic parameters with higher correlation coefficients (Pearson or Spearman coefficients, depending on the study) for determining perfusion-weighted imaging abnormalities are recorded for each study. Nearly all correlations were significant ($P < .05$). The correlation coefficient for mean transit time (MTT) values used to detect perfusion abnormalities in the Schellinger et al study was not available. CBF = cerebral blood flow, rCBF = relative cerebral blood flow, rCBV = relative cerebral blood volume, rMTT = relative mean transit time, T_{max} = time to peak impulse response, TTP = time to peak.

* Numbers in parentheses are reference numbers.

the technique is standardized in the sense that the same ADC cutoff value was used for all patients.

This study had limitations: First, it involved monocentric evaluation, and it has not yet been proved that the method can work with data from different MR imaging systems at other centers. We are currently developing a user-friendly version of the algorithm to

distribute to other centers for evaluation. Note, however, that ADCs are physical measures that are theoretically independent of the MR imaging system with which they are derived. In addition, although this method has been tested with a large series of patients with a wide range of infarct sizes and IG volumes, the ADC cutoff parameters of the image analysis technique were simi-

lar to those suggested in retrospective studies (9,18).

Second, our results were not directly compared with outcomes of perfusion imaging–diffusion imaging mismatching because perfusion-weighted imaging is not systematically performed in all patients at our stroke center owing to time constraints and uncertainties concerning the clinical value of the per-

fusion imaging–diffusion imaging mismatch (12,13). Still, a survey of the literature reveals that these two approaches might perform similarly. Results of studies of perfusion-weighted imaging performed within 12 hours after stroke onset (9,22–33) indicate a significant correlation between acute perfusion-weighted imaging volumes and final infarct volumes in the setting of acute hemispheric stroke. Correlation coefficients have ranged from 0.35 to 0.92 (Table 2), which is consistent with the coefficient of 0.828 derived in our study. Nevertheless, direct comparison with perfusion imaging–diffusion imaging mismatch measures should be investigated in larger multicenter data sets.

Third, V1 and V2 are imperfect estimates of admission and final infarct sizes. The V1 may have been overestimated in some cases because partial reversibility of the admission DW imaging hyperintense signal has been reported (34,35), especially in cases of very early reperfusion. Yet we found the predictive value of the method to be similar when early and late V1 measurements were compared. The described method of measuring V1 could also be criticized because it involves some interactive manual outlining, which is an operator-dependent procedure. Finally, the control MR images were acquired early after stroke and not during the chronic stage. It is our clinical practice to obtain control MR images in patients with acute stroke within 24–48 hours to assess arterial recanalization and IG when the patient is still in the critical care unit. This may have contributed to an overestimation of IG due to edema, especially with large infarcts. However, a longer duration to follow-up MR imaging would have eliminated the cases of severe (fatal) stroke from our study, and measurements obtained during the chronic stages also have limitations, such as an uncontrolled degree of atrophy and fading effects with various MR imaging sequences, which are still poorly understood. On the other hand, V1 and V2 were measured by using the same DW imaging sequence, and from a methodologic point of view, this can be considered an advantage. Finally, the

timing of follow-up MR imaging had no effect on the predictive value of the method.

In general, it will be instructive to verify that the described IG prediction method can also be used to identify the correct voxels in the predicted final lesion compared with the voxels in the true final lesion—even though we found predicted and observed volumes to be strongly correlated. Moreover, further investigations are required to evaluate the specificity and sensitivity of predictions at the level of individual cases.

ADC-based prediction of MCA IG is feasible without intravenous administration of contrast agents. The method is semiautomated, has the potential to be standardized, and might be applied to future stroke trials in which penumbral assessment is required but intravenous contrast material–enhanced perfusion imaging cannot be performed. For future validation, the accuracy of this method at the level of individual predictions needs to be tested and a comparison of this method with the perfusion imaging–diffusion imaging mismatch technique needs to be performed in the same patients.

Acknowledgment: We are grateful to Stéphane Lehericy, MD, PhD, for careful review of the manuscript and helpful suggestions.

References

- Albers GW. Expanding the window for thrombolytic therapy in acute stroke: the potential role of acute MRI for patient selection. *Stroke* 1999;30:2230–2237.
- Albers GW, Thijs VN, Wechsler L, et al. Magnetic resonance imaging profiles predict clinical response to early reperfusion: the Diffusion and Perfusion Imaging Evaluation for Understanding Stroke Evolution (DEFUSE) Study. *Ann Neurol* 2006;60:508–517.
- Warach S. Use of diffusion and perfusion magnetic resonance imaging as a tool in acute stroke clinical trials. *Curr Control Trials Cardiovasc Med* 2001;2:38–44.
- Phan TG, Donnan GA, Davis SM, Byrnes G; and MR Stroke Collaborative Group. Proof-of-principle phase II MRI studies in stroke: sample size estimates from dichotomous and continuous data. *Stroke* 2006;37:2521–2525.
- Barber PA, Parsons MW, Desmond PM, et al. The use of PWI and DWI measures in the design of “proof of concept” trials. *J Neuroimaging* 2004;14:123–132.
- Neumann-Haefelin T, Witsack HJ, Wenserski F, et al. Diffusion- and perfusion-weighted MRI: the DWI/PWI mismatch region in acute stroke. *Stroke* 1999;30:1591–1597.
- Sorensen AG, Buonanno FS, Gonzalez RG, et al. Hyperacute stroke: evaluation with combined multisection diffusion-weighted and hemodynamically weighted echo-planar MR imaging. *Radiology* 1996;199:391–401.
- Lansberg MG, Thijs VN, Hamilton S, et al. Evaluation of the clinical-diffusion and perfusion-diffusion mismatch models in DEFUSE. *Stroke* 2007;38:1826–1830.
- Oppenheim C, Grandin C, Samson Y, et al. Is there an apparent diffusion coefficient threshold in predicting tissue viability in hyperacute stroke? *Stroke* 2001;32:2486–2491.
- Sobesky J, Weber OZ, Lehnhardt FG, et al. Does the mismatch match the penumbra? MRI and PET in early ischemic stroke. *Stroke* 2005;36:980–985.
- Butcher KS, Parsons M, MacGregor L, et al. Refining the perfusion-diffusion mismatch hypothesis. *Stroke* 2005;36:1153–1159.
- Keir SL, Wardlaw JM. Systematic review of diffusion and perfusion imaging in acute ischemic stroke. *Stroke* 2000;31:2723–2731.
- Kane I, Sandercock P, Wardlaw J. Magnetic resonance perfusion diffusion mismatch and thrombolysis in acute ischaemic stroke: a systematic review of the evidence to date. *J Neurol Neurosurg Psychiatry* 2007;78:485–491.
- Hacke W, Furlan A; for the DIAS-2 Investigators. Results from the Phase III Study of Desmoteplase in Acute Ischemic Stroke Trial 2 (DIAS 2) [abstr]. *Cerebrovasc Dis* 2007; 23(suppl 2):54.
- Davis SM, Donnan GA, Parsons MW, et al. Effects of alteplase beyond 3 h after stroke in the Echoplanar Imaging Thrombolytic Evaluation Trial (EPITHET): a placebo-controlled randomised trial. *Lancet Neurol* 2008;7:299–309.
- Detre JA, Zager EL, Alsop DC, Harris VA, Welsh FA. Correlation of diffusion MRI and heat shock protein in a rat embolic stroke model. *J Neurol Sci* 1997;148:163–169.
- Sakoh M, Ostergaard L, Gjedde A, et al. Prediction of tissue survival after middle cerebral artery occlusion based on changes in the apparent diffusion of water. *J Neurosurg* 2001;95:450–458.
- Na DG, Thijs VN, Albers GW, Moseley ME,

- Marks MP. Diffusion-weighted MR imaging in acute ischemia: value of apparent diffusion coefficient and signal intensity thresholds in predicting tissue at risk and final infarct size. *AJNR Am J Neuroradiol* 2004;25:1331-1336.
19. Schaefer PW, Ozsunar Y, He J, et al. Assessing tissue viability with MR diffusion and perfusion imaging. *AJNR Am J Neuroradiol* 2003;24:436-443.
 20. Hevia-Montiel N, Rosso C, Chupin M, et al. Automatic prediction of final infarct growth in acute ischemic stroke from MR apparent diffusion coefficient maps. *Int J Comput Assist Radiol Surg* 2006;1:115-117.
 21. Rosso C, Hevia-Montiel N, Deltour S, et al. A new DWI-based method of MCA infarct growth prediction during the therapeutic window [abstr]. *Stroke* 2007;38(P11):488.
 22. Parsons MW, Yang Q, Barber A, et al. Perfusion magnetic resonance imaging maps in hyperacute strokes: relative cerebral blood flow most accurately identifies tissue destined to infarct. *Stroke* 2001;32:1581-1587.
 23. Schellinger PD, Jansen O, Fiebach JB, et al. Monitoring intravenous recombinant tissue plasminogen activator thrombolysis for acute ischemic stroke with diffusion and perfusion MRI. *Stroke* 2000;31:1318-1328.
 24. Barber PA, Darby DG, Desmond PM, et al. Prediction of stroke outcome with echoplanar perfusion- and diffusion-weighted MRI. *Neurology* 1998;51:418-426.
 25. Beaulieu C, de Crespigny A, Tong DC, Moseley ME, Albers GW, Marks MP. Longitudinal magnetic resonance imaging study of perfusion and diffusion in stroke: evolution of lesion volume and correlation with clinical outcome. *Ann Neurol* 1999;46:568-578.
 26. Rordorf G, Koroshetz WJ, Copen WA, et al. Regional ischemia and ischemic injury in patients with acute middle cerebral artery stroke as defined by early diffusion-weighted and perfusion-weighted MRI. *Stroke* 1998;29:939-943.
 27. Parsons MW, Barber PA, Chalk J, et al. Diffusion- and perfusion-weighted MRI response to thrombolysis in stroke. *Ann Neurol* 2002;51:28-37.
 28. Shih LC, Saver JL, Alger JR, et al. Perfusion-weighted magnetic resonance imaging thresholds identifying core, irreversibly infarcted tissue. *Stroke* 2003;34:1425-1430.
 29. Thijs VN, Adami A, Neumann-Haefelin T, Moseley ME, Albers GW. Clinical and radiological correlates of reduced cerebral blood flow measured using magnetic resonance imaging. *Arch Neurol* 2002;59:233-238.
 30. Rose SE, Janke AL, Griffin M, Finnigan S, Chalk JB. Improved prediction of final infarct volume using bolus delay-corrected perfusion-weighted MRI: implications for the ischemic penumbra. *Stroke* 2004;35:2466-2471.
 31. Derex L, Nighoghossian N, Hermier M, et al. Influence of pretreatment MRI parameters on clinical outcome, recanalization and infarct size in 49 stroke patients treated by intravenous tissue plasminogen activator. *J Neurol Sci* 2004;225:3-9.
 32. Schellinger PD, Fiebach JB, Jansen O, et al. Stroke magnetic resonance imaging within 6 hours after onset of hyperacute cerebral ischemia. *Ann Neurol* 2001;49:460-469.
 33. Röther J, Schellinger PD, Gass A, et al. Effect of intravenous thrombolysis on MRI parameters and functional outcome in acute stroke < 6 hours. *Stroke* 2002;33:2438-2445.
 34. Minematsu K, Li L, Sotak CH, Davis MA, Fisher M. Reversible focal ischemic injury demonstrated by diffusion-weighted magnetic resonance imaging in rats. *Stroke* 1992;23:1304-1310.
 35. Fiehler J, Foth M, Kucinski T, et al. Severe ADC decreases do not predict irreversible damages in humans. *Stroke* 2002;33:79-86.